Vision-based correction of gyroscopic drift in tethered drones

Line Micha Pedersen, Christian Grønborg Madsen, Julian Witold Wagner,
Alexander Singleton Koudal, Adrián Sanchis Reig, Thomas Schou Sørensen
The Technological Faculty for IT og Design
Aalborg University, Aalborg, Denmark
Email: es-23-rob-7-751@student.aau.dk

***Abstract*—Unmanned Aerial Vehicles (UAV) are gaining interest in applications such as surveillance, inspection, or communication, which also encompass a wide range of environments. In the development of UAV-based applications, there arises a significant challenge in their control systems due to the gyroscope, which has potential to be susceptible to considerable levels of noise and bias. Concurrently, introducing a UAV to a GPS-denied environment further complicates localisation, and its ability to correct gyroscopic drift. It is evident that an alternative approach is needed, particularly for tethered UAVs. This paper employs 6 Degrees of Freedom (6-DOF) pose estimation algorithm for a quadcopter UAV from Konomura and Hori [1], utilising a monocular camera for drift alleviation. A system was designed and implemented to test the algorithm, which was done in a lab environment. Testing included what is believed to be critical aspects of the algorithm, i.e. height estimation and stability. However, notable issues become evident, specifically image noise and blur. Furthermore, the algorithm parameters could be optimised in order to achieve higher accuracy, overcoming current limitations.**

Results exhibit promising accuracy within the anticipated margin and despite the aforementioned issues, the algorithm proved to be an interesting approach to alleviating gyroscopic drift.

I. Introduction

In recent years, unmanned aerial vehicles (UAVs) have been gaining interest in the commercial field of mobile robotics due to their broad applicability. Current applications include inspection and surveying [2], [3], surveillance [4], communication[5], teleoperation[6], construction[7] and entertainment[8]. As a consequence, the development of control modalities for these has increased substantially, which require high accuracy due to rapidly changing and hazardous environments. Furthermore, when introducing UAVs to urban- and GPS-deficient environments, localisation can, without additional input, fail or destabilise. These issues are problematic especially for tethered UAVs due to their restricted workspace and possible hazardous outcomes of reaching boundaries.

Hardware and sensory systems applied to UAVs, such as Inertial Measurement Units (IMUs) and microcontrollers, are subject to both weight and computation limitations as size and weight can influence the stability. Furthermore, sensor arrays and sensors in general are often biased or contain noisy output, which can influence the stability of applied control systems.

Gyroscopes are subject to potential bias and drift, which poses an issue in UAVs, as these are most often propeller-driven and heavily rely on accurate pose estimation to remain airborne. This obstacle is also applicable to tethered UAVs, particularly in scenarios where the UAV has to operate in GPS-denied environments, thus the need for alternative or supplementary control schemes is evident. Multiple proposed control modalities attempt at alleviating sensor drift in UAVs, including vision-based solutions [9], [11], a tether-slack based solution [12], and a probabilistic modelling solution [10], which achieves varying amounts of success. Particularly, a study by Konomura and Hori [1] proposes an interesting solution for replacing the accelerometer array, by utilising markers with known global positions and a vision system for 6 Degrees of freedom (DOF) pose estimation. Particularly, this poses a viable solution for alleviating gyroscopic drift.

II. 6-DOF pose estimation algorithm

The method by Konomura and Hori [1] proposes that with a known marker position, a monocular camera can be utilised in substituting an accelerometer array for 6 degrees of freedom (DOF) pose estimation. The algorithm utilises an initial guess of the camera pose to transform the known marker position onto the image plane and employs a minimisation algorithm to iteratively reduce the error between the observed and projected marker positions in the image. Thus, let the camera take on some assumed position $T = [t_x, t_y, t_z]^\intercal \in \mathbb{R}^3$ and orientation $R \in SO(3)$ in a predefined global coordinate system and some markers take up some known position $X_i \in \mathbb{R}^3$ in the same coordinate system. The image area resulting from the position taken up by the quadcopter represents the correct pose of the camera. The position of the observed marker can be expressed as the pixel indices in the image $\mathbf{u_i} = [u_i, v_i]$.

Assuming the camera's relative position estimate is accurate, the position of both the projected- and observed marker should be equal. The error can be described as a reprojection error represented by the L^2-norm between the pixel positions.

$$J = \sum_i ||\mathbf{u_i} - \phi(R, X_i, T)||^2 \tag{1}$$

Where $\phi : \mathbb{R}^3 \mapsto \mathbb{R}^2$ here corresponds to a function mapping from 3D space onto the image plane and J representing the reprojection error. Due to the construction of monocular cameras, the projection of points in 3D space can be described

by a pinhole model, in the previous equation ϕ, here described as:

$$\omega_i \begin{bmatrix} u_i \\ v_i \\ f \end{bmatrix} = R^\intercal X_i - R^\intercal T \tag{2}$$

Thus, by the notion of knowing the position of the ith marker and with the task of minimising the reprojection error in equation 1, a rotation is introduced in equation 2. With the addition of a small rotation $dR \in SO(3)$, the above pinhole model can be expressed as:

$$\omega_i \begin{bmatrix} u_i \\ v_i \\ f \end{bmatrix} = (R + dR)^\intercal (X_i - T) \tag{3}$$

Where dR is defined as:

$$dR = \begin{bmatrix} 0 & -\omega_z & \omega_y \\ \omega_z & 0 & -\omega_x \\ -\omega_y & \omega_y & 0 \end{bmatrix}$$

ω_x, ω_y, and ω_z represent rotations in roll, pitch and yaw respectively. Accordingly, the minimisation variables for the pinhole model are $\xi = [t_x, t_y, t_z, \omega_x, \omega_y, \omega_z]^\intercal \in \mathbb{R}^6$. Due to the non-linearity in determining the derivative of a rotation matrix, the issue is approached using small rotations, as the derivative of the matrix can be assumed to be linear near the initial rotation. Thus, the Levenberg-marquardt algorithm can be applied in an iterative fashion in order to approach an optimal solution for updating R and T,:

$$T \leftarrow\!\shortmid T + \delta T \tag{4}$$

$$R \leftarrow\!\shortmid \exp(\omega \times I) R \tag{5}$$

III. System Implementation

The implemented system utilises the quadcopter with a mounted monocular camera, incorporating a Teensy 4.0 microcontroller for the integration of control systems and sensor communication, alongside a Raspberry Pi for facilitating system-wide communication and image acquisition and processing. System components include a quadcopter and a laptop for more computationally demanding tasks.

A. Drone components

The accurate determination of a drone's position and orientation is paramount for successful navigation and operation. To achieve this, a set of sensors housed within the GY-88 module is employed, including an Inertial Measurement Unit (MPU6050), a Magnetometer (HMC588L), and a Barometer (BMP084). These sensors gather data on the drone's movement, orientation, and altitude. To seamlessly integrate and refine this diverse dataset, an Extended Kalman Filter (EKF) is utilised, ensuring the acquisition of precise and real-time positional information for the drone.

In the process of sensor fusion, the EKF maximises the strengths of each sensor while mitigating their individual limitations. Together, the IMU, magnetometer, barometer, and EKF form a cohesive system, empowering the drone to attain accurate and real-time positional information that remains reliable across diverse environmental conditions.

B. Image Acquisition and Processing

In order to set up the vision system, a Raspberry Pi V2.1 with an IMX219 sensor is connected to the Raspberry Pi. To represent four LED lights, a piece of paper is marked with four different coloured circles, with the colours being red, blue, green, and yellow as seen in figure 1.

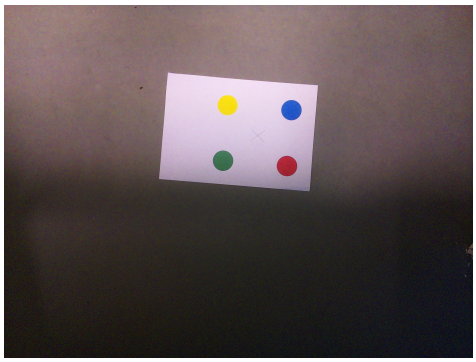

Fig. 1: Picture of the markers captured by the Picam V2.1

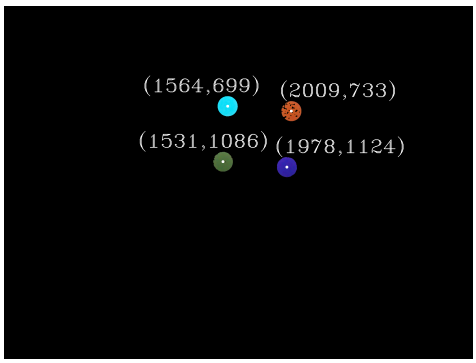

Fig. 2: Picture from Picam V2.1 masked in HSV colour space. The centre of each marker represented by the white dots is calculated, and the pixel coordinates are written above each marker.

When the vision program starts, a picture of the paper is captured. The RGB values are converted to HSV values. HSV colour space is used instead of RGB as it is more invariant to lighting changes in terms of defining the boundaries of the four different colours. The picture is masked to isolate each marker after which the centre of each marker is calculated. A representation of the masking in HSV and the calculated centre points are shown in figure 2.

C. Algorithm implementation

The estimation algorithm is executed on the laptop alongside the other system processes, receiving data from the sensor array along with the calculated centre positions of the markers for initial guesses of translation and rotation. The known marker positions are predefined in the system, the results are then iteratively optimised and sent along to the EKF, for refining the general position estimate.

D. Control System

The control system is designed and validated based on a simplified model in Simulink. A drone was simulated in six degrees of freedom, utilising Aerospace block 6DOF. Therefore, six states of the drone have been tracked: X, Y, Z position, roll, pitch, and yaw. Equations of motion for the drone were linearised around the hovering state. Additionally, linear relation of lift and moment created by motors.

$$\mathbf{F} = C_L \cdot \omega^2$$
$$\mathbf{M} = C_M \cdot \omega^2$$

The coupling of the X position and pitch of the drone is been taken advantage of for position control. A similar coupling effect is used to control the position on the Y-axis and roll. Two cascaded PID controllers is created for those four states. Additionally, one controller each for the remaining states is introduced to the system. PID gains were firstly obtained by using built-in auto-tuning in Simulink. After satisfactory results, all controllers are implemented on Teensy, and the control system was again tested in a lab environment. Additional adjustments are made to PID gains as the simplified simulated environment does not take into account other external factors.

$$\begin{bmatrix} \omega_1^2 \\ \omega_2^2 \\ \omega_3^2 \\ \omega_4^2 \end{bmatrix} = \begin{bmatrix} C_L \cdot D & -C_L \cdot D & C_L \cdot D & -C_L \cdot D \\ C_L \cdot D & C_L \cdot D & -C_L \cdot D & -C_L \cdot D \\ -C_M \cdot R & C_M \cdot R & C_M \cdot R & -C_M \cdot R \\ -C_L & -C_L & -C_L & -C_L \end{bmatrix}^{-1} \cdot \begin{bmatrix} \mathbf{M_x} \\ \mathbf{M_y} \\ \mathbf{M_z} \\ \mathbf{F_z} \end{bmatrix}$$

In order to calculate the required speed of the motors, the output forces and moments calculated by the controller are multiplied by the control matrix. The output is being processed to obtain a PWM signal, which is then sent to motors.

IV. Testing

Testing the system is performed with the purpose of evaluating the accuracy and limitations of the proposed algorithm fused with sensor data and vision algorithm. Testing is conducted in a lab environment in order to directly identify discrepancies in the algorithm's performance in relation to the above-mentioned issues when used with a monocular camera. Thus, executing the system in different scenarios where the system output is expected to change.

A. Height estimation

The height estimation is a crucial aspect of the drone's performance, particularly as it relies on a camera-based system for estimation. Therefore, the ability of the system to correctly estimate altitude is evaluated. The system should theoretically be robust, even for small changes in altitude, thus the testing scenarios include a multitude of distinct altitudes ranging from 1 to 3 meters, in 0.5 meter increments. These altitudes were chosen to represent a spectrum of typical flight scenarios in indoor environments, thus accommodating a lab environment. Furthermore, the lab environment ensures that no outside factors influence the results.

The vision sensor attached to the quadcopter features a pixel resolution of 3280×2464. Consequently, when discretising distances, such as in the case of a 10-meter interval, each pixel represents a remarkably fine resolution of 1.8 mm both vertically and horizontally. Therefore, the expected variation in estimated height is assumed to achieve moderately accurate results, with minuscule variance. However, for a realistic testing scenario taking into account factors such as noise and unintended quadcopter movement, this assumption is potentially inaccurate.

The altitude calculation involves not only the camera-based system but also incorporates data from the IMU (Inertial Measurement Unit) and the pressure sensor. It's worth noting that these additional components can be sensitive to external factors, further complicating the challenge of maintaining precise altitude estimates.

To conduct a comprehensive assessment, experiments are executed within a controlled environment featuring fixed marker positions and a designated take-off area for the quadcopter. Each altitude is individually tested to discern the influence of height on measurement accuracy. To establish ground truth measurements, a marker-based motion capture system is employed, outfitting the quadcopter with an infrared marker for accurate localisation. This approach ensures a reliable reference point against which the accuracy of the altitude estimation system can be benchmarked.

1) Results: The expected results for this test are assumed to deviate slightly due to noise from other parts of the system but stay within a margin of about 2% error.

B. Stability

The stability test should evaluate the performance of our localisation algorithm, EKF, and control system in mitigating gyroscopic drift for the tethered UAV. Two tests are conducted with different time durations, one for 5 minutes and another for 10 minutes, to assess the system's stability under varying operational conditions.

The stability test is carried out in a controlled environment, similar to the one used for the height estimation tests. The quadcopter is attached to a fixture to prevent it from unintended movement or crashing, allowing the evaluation of internal stability mechanisms. The test involves continuous operation of the quadcopter for the specified durations. Throughout the test, the position, and orientation estimates

from the localisation algorithm and EKF are compared against the ground truth obtained from the marker-based motion capture system. The ability of the control system to counteract gyroscopic drift is evaluated by analysing the consistency of the estimated position and orientation over time.

To induce controlled disturbances and simulate real-world conditions, external forces are applied at specific intervals during the test. These disturbances could include variations in tether tension or intentional manual movements of the drone. These perturbations allow for an assessment of the system's resilience in maintaining stability and recovering from external influences.

Sensor data, including gyroscopic measurements, accelerometer readings, and other localisation information, are logged throughout the test duration. The collected data is then analysed to quantify any deviations from the expected position and orientation over time. The stability of the system is assessed by considering factors such as drift rate, error accumulation, and the responsiveness of the control system to disturbances.

V. Results

The expected results for the stability test include an analysis of the system's ability to maintain accurate position and orientation estimates over the specified durations. The evaluation considers factors such as drift magnitude, the speed of error accumulation, and the effectiveness of the control system in correcting deviations.

It is anticipated that the system will exhibit a stable performance within the defined timeframes, with minor deviations due to inherent noise and external disturbances. The results will provide insights into the robustness of the localisation algorithm, EKF, and control system in ensuring the stability of the tethered UAV during extended operation. Any observed deviations will be analysed to identify potential improvements in the system's stability mechanisms.

VI. Discussion

Based on these results, it is evident that some parameters should be tuned in order to improve system performance in general. However, image acquisition and processing is also contributing to errors. This can be attributed to noise, blurring, or sensor resolution collectively. In the current implementation, image noise can result in failure to determine marker centre points, resulting in a skewed or distorted transform. Similarly, image blur from rapid spontaneous movement can also result in incorrect marker localisation. Due to its inherent discretisation of distance, the error could be attributed to the resolution of the monocular camera. However, this poses an issue to systems that require image processing. Higher resolutions require more processing time, resulting in lower update frequency in relation to the vision-based sensor drift alleviation. Evidently, the choice of sensor is a compromise between sensor resolution and algorithm operation frequency.

Furthermore, the presented results reveal an issue with the altitude of the monocular camera. Due to discretisation, the length each pixel represents increases at higher altitudes, leading to a lower output resolution relative to the algorithm. This is an issue for the stability of the system, thus the camera resolution must be determined for a specific height, and output resolution in order for the algorithm to pose a viable solution to gyroscopic sensor drift.

Additionally, the accuracy of the algorithm could be improved, as discussed by Konommura and Hori [1], by utilising non-co-planar markers, as the influence of movement and rotation becomes more apparent with markers placed at different altitudes. Furthermore, marker design might also increase system reliability, as markers, depending on design, might be more easily distinguishable in cluttered environments or unknown environments.

VII. Conclusion

A proposition for 6-DOF pose estimation using EKF and an iterative reprojection minimisation algorithm for co-planar coloured markers is presented. The system is employed for the alleviation of gyroscopic drift in quadcopter UAVs utilising a monocular camera. A control system has been designed and implemented for testing the algorithm alongside sensor measurements. Tests have been conducted to showcase both the advantages and the shortcomings of this type of system. It is evident, that improvements and potential estimation algorithms for distance discretisation in pixels could further improve the accuracy of the utilised algorithm.

References

[1] R. Konomura and K. Hori, *FPGA-based 6-DoF pose estimation with a monocular camera using non co-planer marker and application on micro quadcopter,* 2016 IEEE/RSJ International Conference on Intelligent Robots and Systems (IROS), Daejeon, Korea (South), 2016, pp. 4250-4257, doi: 10.1109/IROS.2016.7759626.

[2] Jordan, S., Moore, J., Hovet, S., Box, J., Perry, J., Kirsche, K., Lewis, D. and Tse, Z.T.H. (2018), State-of-the-art technologies for UAV inspections. IET Radar Sonar Navig., 12: 151-164. https://doi.org/10.1049/iet-rsn.2017.0251

[3] Christiansen, M.P.; Laursen, M.S.; Jørgensen, R.N.; Skovsen, S.; Gislum, R. Designing and Testing a UAV Mapping System for Agricultural Field Surveying. Sensors 2017, 17, 2703. https://doi.org/10.3390/s17122703

[4] E. Semsch, M. Jakob, D. Pavlicek and M. Pechoucek, "Autonomous UAV Surveillance in Complex Urban Environments," 2009 IEEE/WIC/ACM International Joint Conference on Web Intelligence and Intelligent Agent Technology, Milan, Italy, 2009, pp. 82-85, doi: 10.1109/WI-IAT.2009.132.

[5] Bander Alzahrani, Omar Sami Oubbati, Ahmed Barnawi, Mohammed Atiquzzaman, Daniyal Alghazzawi, UAV assistance paradigm: State-of-the-art in applications and challenges, Journal of Network and Computer Applications, Volume 166, 2020, 102706, ISSN 1084-8045, https://doi.org/10.1016/j.jnca.2020.102706.

[6] Wen, Ming-Chang, et al. "A Stereo Vision-based support system for teleoperation of unmanned vehicle." ISARC. Proceedings of the International Symposium on Automation and Robotics in Construction. Vol. 32. IAARC Publications, 2015.

[7] Masiri Kaamin, Siti Nooraiin Mohd Razali, Nor Farah Atiqah Ahmad, Saifullizan Mohd Bukari, Norhayati Ngadiman, Aslila Abd Kadir, Nor Baizura Hamid; The application of micro UAV in construction project. AIP Conf. Proc. 3 October 2017; 1891 (1): 020070. https://doi.org/10.1063/1.5005403

[8] Abdelkader, M., Güler, S., Jaleel, H. et al. Aerial Swarms: Recent Applications and Challenges. Curr Robot Rep 2, 309–320 (2021). https://doi.org/10.1007/s43154-021-00063-4

[9] C. Demonceaux, P. Vasseur, and C. Pégard, Robust attitude estimation with catadioptric vision, IEEE International Conference on Intelligent Robots and Systems, pp. 3448–3453, 2006. DOI: 10.1109/IROS.2006.282585

[10] A. Al-Radaideh and L. Sun, "Observability Analysis and Bayesian Filtering for Self-Localization of a Tethered Multicopter in GPS-Denied Environments," 2019 International Conference on Unmanned Aircraft Systems (ICUAS), Atlanta, GA, USA, 2019, pp. 1041-1047, doi: 10.1109/ICUAS.2019.8797913.

[11] S. Ahrens, D. Levine, G. Andrews and J. P. How, "Vision-based guidance and control of a hovering vehicle in unknown, GPS-denied environments," 2009 IEEE International Conference on Robotics and Automation, Kobe, Japan, 2009, pp. 2643-2648, doi: 10.1109/ROBOT.2009.5152680.

[12] S. Kiribayashi, K. Yakushigawa and K. Nagatani, "Position estimation of tethered micro unmanned aerial vehicle by observing the slack tether," 2017 IEEE International Symposium on Safety, Security and Rescue Robotics (SSRR), Shanghai, China, 2017, pp. 159-165, doi: 10.1109/SSRR.2017.8088157.